Dalton Transactions

RSC Publishing

PAPER

View Article Online
View Journal | View Issue

Cite this: *Dalton Trans.*, 2013, **42**, 14309

Seed-mediated growth of jack-shaped gold nanoparticles from cyclodextrin-coated gold nanospheres†

Alfredo Sánchez,[a] Paula Díez,[a] Reynaldo Villalonga,*[a,b] Paloma Martínez-Ruiz,[c] Marcos Eguílaz,[a] Iñigo Fernández[a] and José M. Pingarrón*[a,b]

Received 27th May 2013,
Accepted 30th July 2013

DOI: 10.1039/c3dt51368h

www.rsc.org/dalton

Branched gold nanoparticles were prepared by a seed-mediated approach using per-6-thio-6-deoxy-β-cyclodextrin capped gold nanospheres as seeds and a growth medium similar to those commonly employed to prepare gold nanorods, containing $AgNO_3$, ascorbic acid and cetyltrimethylammonium bromide. Novel jack-shaped gold nanoparticles (102–105 nm) were obtained at a specific range of Ag^+ ion concentrations (62–102 μM). The crystalline structure of these nanoparticles was confirmed by high-resolution transmission electron microscopy. The influence of the perthiolated β-cyclodextrin on the successful preparation of gold nanojacks was demonstrated. The jack-shaped gold nanoparticles showed strong absorption in the near infrared region and excellent catalytic activity for the electrochemical oxidation of H_2O_2.

Introduction

The synthesis of metal nanoparticles with defined morphology has attracted broad research interest and has undergone rapid development due to the unique electronic, optical, chemical and electrochemical properties of these nanomaterials.[1] In particular, a great deal of effort has been devoted to the development of methods for preparing branched and star-shaped gold nanoparticles.[2–7] These anisotropic nanomaterials show strong absorption in the near-infrared region, allowing their biomedical application as efficient contrast agents for biological tissues and cell imaging. Branched and star-shaped gold nanoparticles also show enhanced electromagnetic field intensity at their tip apexes, yielding higher signals in surface-enhanced Raman spectroscopy and thus favoring ultrasensitive detection.

Nanostars can be synthesized through a variety of seedless[5–7] and seed-mediated wet approaches[2–4] in aqueous and organic media, using diverse gold reducing conditions. In general, seed-mediated methods are preferred due to the possibility of using a great variety of nanoparticle seeds with different morphologies as well as the higher size- and shape-control of the nanostar growth.[8–12] As a general rule, the seed-mediated synthesis of branched gold nanostructures requires the use of selective capping agents during the colloid growth, due to the symmetric face-centered cubic lattice of gold nanoparticles.[8] In this regard, surfactants, DNA and polymers have been extensively employed as molecular templates for the sterically induced shape control of gold nanostar synthesis through seed-mediated strategies.[2–4,8–12] In addition, the type of reducing agent and the presence or absence of silver ions are also key factors in the rational syntheses of branched gold nanostructures.[1]

The surfactant cetyltrimethylammonium bromide (CTAB) combined with silver ions have been the capping agents more commonly employed to prepare anisotropic gold nanostructures. Nehl *et al.* used this capping mixture to prepare star-shaped gold nanoparticles of about 100 nm in high yield.[8] Vigderman and Zubarev described the synthesis of star fruit-shaped gold nanorods by using pentahedrally twinned gold nanorods as seeds.[13] Highly branched gold nanoparticles with controlled morphology were prepared by Sau and Murphy by using specific concentrations of CTAB, $AgNO_3$ and ascorbic acid as a reductant.[9]

Cyclodextrins are macrocyclic compounds with shallow truncated cone shapes usually employed as templates for the synthesis of polymeric and inorganic materials.[14] Cyclodextrins,[15] as well as their mono- and perthiolated derivatives,[16–18] have been also employed as ligands for the synthesis of water-

[a]*Department of Analytical Chemistry, Faculty of Chemistry, Complutense University of Madrid, 28040-Madrid, Spain. E-mail: pingarro@quim.ucm.es, rvillalonga@quim.ucm.es; Tel: +34 913944315*
[b]*IMDEA Nanoscience, Cantoblanco Universitary City, 28049-Madrid, Spain*
[c]*Department of Organic Chemistry I, Faculty of Chemistry, Complutense University of Madrid, 28040-Madrid, Spain*
†Electronic supplementary information (ESI) available. See DOI: 10.1039/c3dt51368h

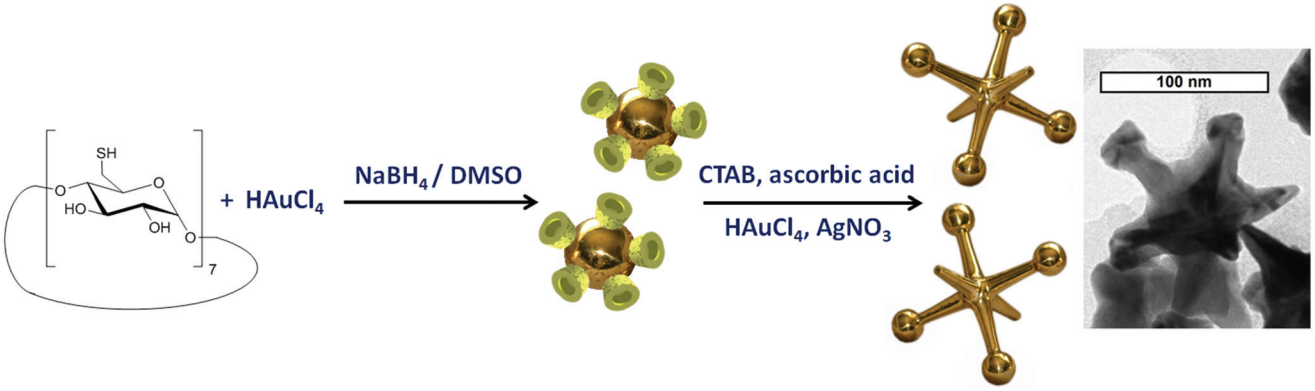

Scheme 1 Preparation of jack-shaped gold nanoparticles.

soluble gold nanoparticles. Special interest has been devoted to the latter cyclodextrin-coated gold nanostructures due to their molecular receptor properties. However, the use of cyclodextrins as capping agents for the preparation of branched noble metal nanoparticles has not been reported to date. In this communication, a novel template-based approach to prepare anisotropic jack-shaped gold nanoparticles by using β-cyclodextrin (βCD) coated gold nanospheres as seed material is described (Scheme 1).

Experimental

Reagents and apparatus

β-Cyclodextrin, CTAB, $HAuCl_4$ and all other chemicals were purchased from Sigma (USA).

Transmission electron microscopy (TEM) and high resolution transmission electron microscopy (HRTEM) measurements were performed using JEOL JEM-2000 FX and JEOL JEM-3000 F microscopes, respectively (Jeol Ltd, Japan). Spectrophotometric measurements were performed using an Agilent 8453 UV/VIS spectrophotometer (Hewlett Packard, USA). Cyclic voltammetry was performed using a FRA2 μAutolab Type III potentiostat/galvanostat and the data were acquired using the GPES Ver. 4.9 and Frequency Response Analyser software, respectively (Metrohm Autolab B.V., The Netherlands).

Synthesis of βCD-coated gold nanoparticles

Mono-6-ethylenedithiol-6-deoxy-βCD (βCD-SH_1) was prepared by dissolving 900 mg of mono-6-tosyl-6-deoxy-βCD[19] in 47 mL of 0.5% (w/v) Na_2CO_3 in 20% (v/v) ethanol solution. Three mL of 1,2-ethanedithiol were further added and the reaction mixture was stirred for 48 h. The mixture was then added to 200 mL of a 4 : 1 (v/v) EtOH–Et_2O solution, and the resulting precipitate was filtered and exhaustively washed with EtOH and Et_2O. The solid was re-dissolved in acidified water, precipitated, washed again and, finally, dried under vacuum.

Per-6-thio-6-deoxy-βCD (βCD-SH_7) was synthesized as previously reported.[20] The βCD-capped gold nanoparticles were prepared as described[17] using βCD-SH_7 and βCD-SH_1 as capping molecules and a 1 : 5 CD : $AuCl_4^-$ molar ratio.

Synthesis of branched gold nanoparticles

Gold nanostructures were prepared by a modification of the conventional method used to synthesize gold nanorods,[21] but using βCD-SH_7 capped gold nanospheres (Au-βCD-SH_7) as seeds. 50 mL of 0.2 M cetyltrimethylammonium bromide (CTAB) were mixed with 40 mL of milliQ water and 5.0 mL of 5.0 mM $HAuCl_4$ at 25 °C. To these solutions, 700 μL of 79 mM ascorbic acid were added, the colour of the growth solutions rapidly changing from yellow to colourless. Then, different aliquots of a 4 mM $AgNO_3$ solution (0, 0.5, 1.5, 2.5, 3.5 mL) were added to different mixtures. Thereafter, 120 μL of a 1.7 mg mL^{-1} aqueous solution of the Au-βCD-SH_7 were added to the growth solutions, which were kept under magnetic stirring at 25 °C for 120 min. For kinetics experiments, 5 mL aliquots were removed at scheduled times and treated with 3 μL of 3-mercaptopropionic acid.

A similar approach was employed to prepare branched nanoparticles by using βCD-SH_1 coated Au nanoparticles as seeds and 102 μM $AgNO_3$ concentration.

Electrocatalytic oxidation of H_2O_2

Twenty milliliters of a 0.1 mg mL^{-1} aqueous dispersion of the branched gold nanoparticles were dropped on carbon screen-printed electrodes (DropSens, Spain). After drying, the electrodes were washed and evaluated for cyclic voltammetry in 0.1 M sodium phosphate buffer, pH 7.0, in the absence and presence of 1.0 μM H_2O_2.

Results and discussion

Gold colloids were first grown in the presence of perthiolated βCD[17] yielding dark red and water soluble nanospheres (AuCD-SH_7), in which per-6-thio-6-deoxy-βCD was chemisorbed to the as-growing Au colloids through all the seven thiol groups located on the primary oligosaccharide face, then covering completely the surface of the nanoparticles.[17] AuCD-SH_7

showed small average diameter and narrow size distribution of 3.4 ± 0.8 nm. These features allowed the use of AuCD-SH_7 as good candidates for the further seed-mediated overgrowth of more complex gold nanostructures. For this purpose, a similar growth solution to that employed to prepare gold nanorods,[21] involving an aqueous CTAB solution containing ascorbic acid, $AuCl_4^-$ ions and $AgNO_3$, was evaluated. Considering that gold nanoparticles exhibit strong surface plasmon resonance absorption that is dependent on their shape and size, the as-prepared nanoparticles were characterized by UV-Vis-NIR spectroscopy. Fig. 1 shows the normalized spectra for nanoparticles grown at different $AgNO_3$ concentrations during a fixed time interval of 120 min. This time interval was selected since the absorption band of branched gold colloids reached saturation values after this period (data not shown). Initial AuβCD-SH_7 nanoparticles showed only one visible absorption band around 520 nm (Fig. 1, curve a) characteristic of spherically-shaped gold colloids. Nanoparticles grown in the absence of Ag^+ ions yielded red-colored gold colloids (NP0 sample) showing a single and narrow absorption band (Fig. 1A, curve b) which was slightly shifted to around 540 nm with respect to the seeds, indicating the formation of roughly quasi-spherical nanoparticles. This fact was confirmed by TEM revealing that penta- and hexa-twinned nanoparticles with an average size of 54 ± 8 nm were mainly produced (Fig. 1B). Additionally, some nanorods and nanotriangles were also observed. Similar results were previously described for the seed-mediated growth of gold nanoparticles in surfactant media without the addition of silver ions.[2] Size distributions of all the nanoparticles prepared are provided in Fig. 1S in ESI.†

A more significant red-shift in the absorption band occurred for nanoparticles grown in the presence of 21 μM $AgNO_3$ (NP1 sample), with a maximum at 648 nm (Fig. 1A, curve c). The spectrum of these nanoparticles was characterized by a broad and intense absorption band with a secondary and small shoulder band in the near infrared region, with a maximum around 1010 nm. According to this pattern it could be expected that these nanoparticles should have a non-spherical shape, as well as some elongations or distortions on their surface. These bands of the branched nanoparticles can be ascribed to dipole resonances either at the tips or the central core of the nanoparticles.[22,23] As revealed by TEM, star-shaped nanoparticles with penta- and hexaploid morphology were obtained (Fig. 2C). The average circular diameter of the branched nanoparticles, obtained by measuring the length from a branch edge to another one on the opposite side, was estimated to be 103 ± 18 nm.

Jack-shaped nanoparticles with large tip ends with ball-rounded structures could be prepared by seed-mediated growth of AuβCD-SH_7 at higher $AgNO_3$ concentrations of 62 μM (NP2 sample) and 102 μM (NP3 sample), as is illustrated in Fig. 1D and E. Gold nanostars without or with a few ball-rounded tips were also observed in both samples. Average circular diameters of 102 ± 19 nm and 105 ± 15 nm, as well as average lengths for the tips of 42 ± 8 nm and 46 ± 10 nm, were estimated for the NP2 and NP3 nanoparticles, respectively. The average diameters of the ball-rounded structures at the tips were 17 ± 3 nm and 14 ± 4 nm, respectively.

The spectra of the jack-shaped nanoparticles (Fig. 1A, curves c, d) showed a primary absorption band at 605 nm, which could be attributed to dipole resonance located at the branching points. In addition, a broad secondary band in the

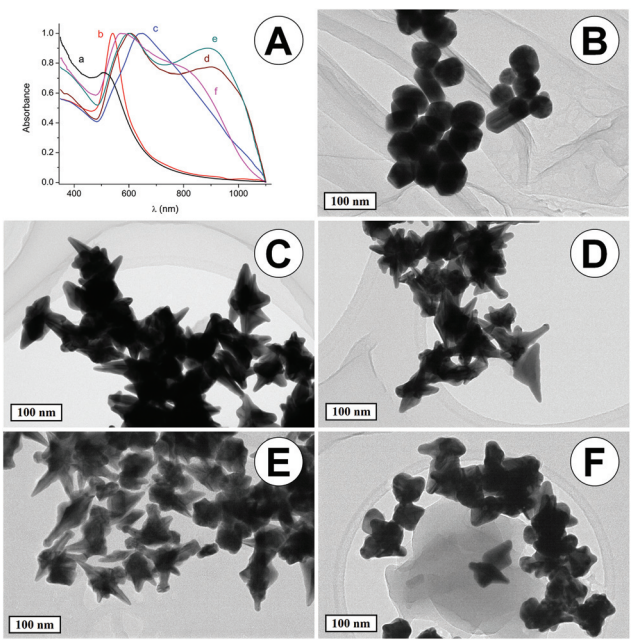

Fig. 1 (A) Normalized UV-Vis spectra recorded for AuβCD-SH_7 (a), NP0 (b), NP1 (c), NP2 (d) NP3 (e) and NP4 (f) nanoparticles. (B–F) TEM images of NP0 (B), NP1 (C), NP2 (D), NP3 (E) and NP4 (F) nanoparticles.

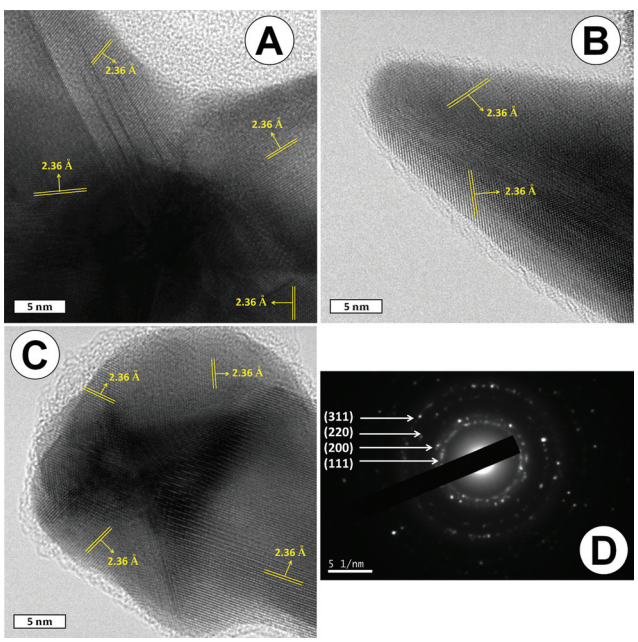

Fig. 2 HR-TEM images (A–C) and SAED analysis (D) of NP3 nanojacks.

near infrared region around 900 nm was observed, which could be ascribed to the longitudinal plasmon resonance at the tips.

Jack-shaped nanoparticles with ball-rounded tips were not observed when a higher $AgNO_3$ concentration of 140 μM was used in the growth medium (NP4 sample). Instead, gold nanostars (82 ± 14 nm) with bulky cores and small protuberances were obtained (Fig. 1F). Accordingly, the spectrum of this sample showed two absorption bands at 575 nm and 812 nm. This blue-shift agrees with a previous report demonstrating that the wavelength of the longitudinal plasmon resonance peak in gold nanostars decreases as the branch-length decreases.[14] At this point, it can be suggested that the formation of jack-shaped nanoparticles is directly affected by the presence of Ag^+ ions at a defined concentration.

The NP3 jack-shaped nanoparticles were characterized by high-resolution TEM (Fig. 2). The core, tips and ball-rounded structures at the tip ends of the nanoparticles mainly contain crystalline lattice planes with a *d*-spacing of 2.36 Å for adjacent lattice planes, corresponding to the (111) planes of face-centered cubic gold. These lattice planes were separated by twin boundaries. The crystalline structure of NP3 nanoparticles was confirmed by selected area electron diffraction (SAED) analysis (Fig. 2D), which clearly showed the characteristic concentric ring patterns with sequences corresponding to a face-centered cubic structure.

Two control experiments were carried out to demonstrate that the sterically induced shape controlled formation of jack-shaped nanoparticles was mediated by the presence of a perthiolated βCD derivative as a capping ligand in the seeds. The first control experiment was a second growth of gold nanoparticles carried out using NP3 particles as seeds under the same growth conditions used for NP3 preparation. The normalized UV-Vis spectrum of the grown nanoparticles showed a broad absorption band at 635 nm, with two minor shoulder bands at 560 nm and 930 nm (Fig. 3A, curve b), suggesting the presence of branched nanostructures with different morphologies. This was confirmed by TEM analysis, revealing the presence of large and polydisperse gold nanoparticles with bulges (167 ± 40 nm) instead of gold nanojacks (Fig. 3B).

Gold nanoparticles coated with mono-6-ethylenedithiol-6-deoxy-βCD (AuβCD-SH_1) were further used as seeds in the second control experiment. The average size of these nanoparticles was estimated to be 3.6 ± 0.5 nm, according to HRTEM measurements (Fig. 4A). Energy Dispersive Spectroscopy (EDS, Fig. 4D) and elemental analysis revealed that the amount of oligosaccharides attached to the two different seeds was about 11 and 12 molecules of βCD in AuβCD-SH_7 and AuβCD-SH_1, respectively, by assuming that the nanoparticles are perfect spheres. This result agrees with previous reports describing the quantification of βCD in AuβCD-SH_7 nanoparticles by the redissolution method.[18]

In this case, the monothiolated βCD derivative is chemisorbed to the Au nanoparticles through the single thiol group at the primary βCD face. Taking into account the similar degree of surface coverage in both AuβCD-SH_7 and AuβCD-SH_1 nanoparticles, it is expected that the latter may provide more active sites for Au reduction during the nanostar growth due to lower steric hindrance to the seed surface. In fact, AuβCD-SH_7 and AuβCD-SH_1 can be attached to the gold surface by seven and one linking points, respectively, thus allowing AuβCD-SH_1 moieties to be assembled in a more free arrangement.

The nanoparticles grown from AuβCD-SH_1 nanoparticles showed two absorptions bands in the UV-Vis spectrum, which are characteristics of branched nanostructures (Fig. 3C, curve c). TEM analysis revealed that star-shaped nanoparticles with

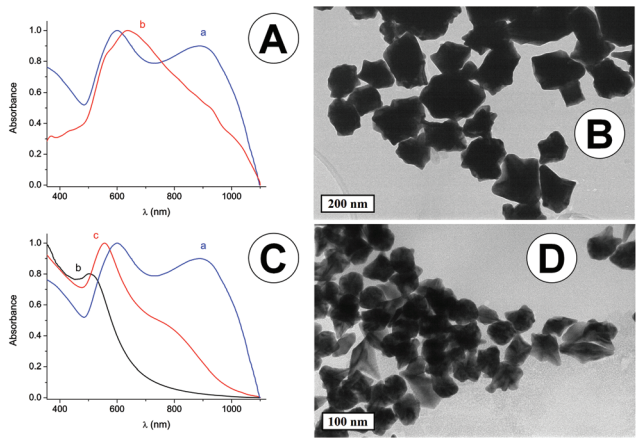

Fig. 3 (A) Normalized UV-Vis spectra of NP3 (a) and gold nanoparticles obtained by the second growth of NP3 under the same growing conditions (b). (B) TEM image of gold nanoparticles obtained by the second growth of NP3. (C) Normalized UV-Vis spectra of NP3 (a), AuβCD-SH_1 (b) and gold nanoparticles obtained by using AuβCD-SH_1 as seeds. (D) TEM image of gold nanoparticles obtained by using AuβCD-SH_1 as seeds.

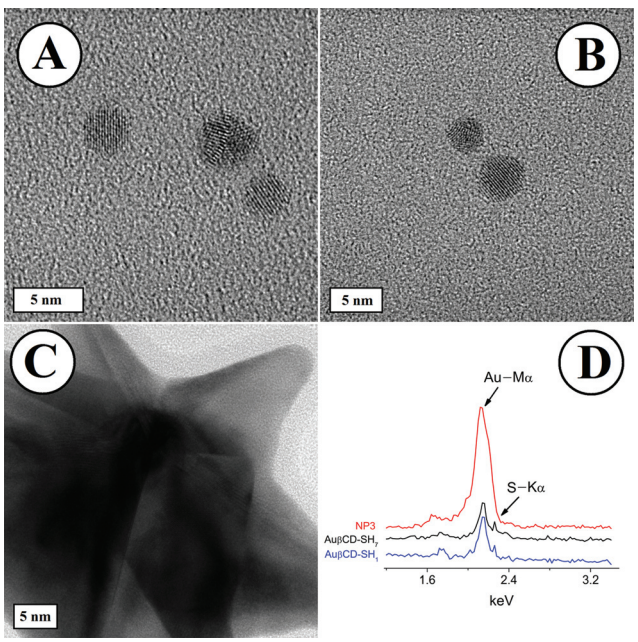

Fig. 4 HRTEM images of AuβCD-SH_1 (A), AuβCD-SH_7 (B) and NP3 nanojacks (C). EDS analysis of these nanoparticles (D).

penta- and hexaploid morphology and short branches were mainly obtained, instead of jack-shaped nanoparticles.

These results evidenced that the preparation of jack-shaped nanoparticles depends on the use of per-6-thio-6-deoxy-βCD as a capping ligand for the Au seeds. However, the difference of the growth processes observed in the presence of mono and perthiolated βCD could be either ascribed to: (1) different structures of the synthesized seeds, and/or (2) the steric effect caused by the capping βCD derivatives during the seed-mediated growth. To elucidate whether the effect of the capping agent originates from the synthesis of the seeds, or later during the growth process, HRTEM analysis of the perthiolated and monothiolated βCD-coated seeds was performed. As illustrated in Fig. 4, both seeds showed spherical geometry and similar diameters, with the characteristic symmetric face-centered cubic lattice of gold nanoparticles. Additionally, both seeds showed similar βCD content. Thus, it is expected that the different branched nanostructures prepared from these seeds could be caused by the different arrangement of the βCD moieties on the seed surface.

There are several theories related to the formation of anisotropic gold nanoparticles by seed-mediated growth in the presence of CTAB/$AgNO_3$.[1,21,24–27] However, all of them are focused on the face-specific capping of the metallic surface by different adducts, which cause the controlled nucleation of growth anisotropy at multiple sites on the non-homogeneously capped seed. For example, it has been postulated that a silver(I) bromide complex (either $AgBr_2^-$ or CTA–Ag–Br^+) acts as a face-specific capping agent, favoring anisotropic growth.[26] Other studies have proposed that silver underpotential deposition on the seed surface may be responsible for directing anisotropic growth.[24,25] On the other hand, it has been hypothesized that CTAB, as well as other long chain surfactants with halide anions, preferentially coat and protect the (100) face of the crystalline gold seed, allowing the anisotropic growth of the nanostructure by deposition of gold on the (111) face.[21,27]

In the present work, the importance of $AgNO_3$ in the formation of star- and jack-shaped nanoparticles is evident. In the absence of silver ions, the nanoparticle growth is kinetically controlled,[1] yielding unbranched nanostructures in the presence of CTAB (Fig. 1B). The addition of silver ions to the growth medium caused a specific surface passivation effect, probably due to silver underpotential deposition or binding of a silver(I) bromide complex, which promotes anisotropic growth. In our case, it could be expected that the metal active surface of the seeds was partially masked by the attached βCD thiol derivatives. The presence of these thiolated hydrophilic oligosaccharide templates should affect the specific passivation of the surface by the silver/CTAB capping agents, producing non-homogeneously capped surfaces and probably promoting the anisotropic growth of rounded and non-rounded tips in the jack-shaped nanoparticles (Fig. 2C–E).

This template-controlled surface passivation was less observed when large silver concentration or monothiolated βCD derivatives were employed, yielding gold nanostars with small protuberances (Fig. 2F and 3D).

As Fig. 4D illustrates, EDS analysis revealed the presence of sulfur in both AuβCD-SH_7 and AuβCD-SH_1 seeds. However, no evidence of this element was detected in NP3 nanoparticles similarly to for the rest of the branched nanostructures (data not shown). This fact suggests that the thiolated βCD moieties were either released from the branched nanostructures or remained there but in very low content with respect to Au.

The potential application of the branched gold nanoparticles for the electrocatalytic oxidation of H_2O_2 was evaluated by cyclic voltammetry with carbon screen-printed electrodes modified with these nanomaterials (Fig. 2S in ESI†). In fact, determination of H_2O_2 is important for electrochemical biosensing because H_2O_2 is produced by several oxidases with analytical relevance.[28] The oxidation of H_2O_2 at the surface of the unmodified electrode was apparent at potential values higher than 600 mV, while remarkably larger anodic current values with a noticeable reduction of the overpotential for the electrochemical reaction were observed for all the nanoparticle-coated electrodes. Among these, lower electrocatalytic activity was noticed for the electrode modified with AuβCD-SH_7 seeds, which could be ascribed to lower active surface area in the nanoparticles due to coverage with the oligosaccharide moieties. An increased electrocatalytic activity was shown by nanoparticles prepared in the absence of silver ions (NP0 sample), as well as for those containing small protuberances (NP4 sample). Moreover, higher electrocatalytic activity toward H_2O_2 oxidation was observed for highly branched nanoparticles containing large protuberances (NP1–NP3 samples). This effect was especially noticeable for NP3 sample, showing very large anodic current values and a significant reduction of the overpotential for the electrochemical oxidation (starting at a potential value of 205 mV). These results evidenced the electrocatalytic activity of the branched nanoparticles toward H_2O_2, probably caused by the occurrence of local overpotential effects at the highly active tip surfaces.

It should be mentioned that the electrocatalytic activity of these nanoparticles could be affected by the presence of residual CTAB molecules, which have a detrimental effect on the electrochemical behavior of electrode surfaces.[29] In fact, adsorption of surfactants on electrode architectures might significantly change the redox potential, charge transfer coefficients and diffusion coefficients of electrode processes.[30]

Conclusions

In summary, here we reported the shape-controlled seed-mediated synthesis of jack-shaped gold nanoparticles by using cyclodextrin-capped gold nanospheres as seeds. The preparation of these novel branched nanostructures is dependent on the presence of Ag^+ ions at a defined concentration in the growth medium, as well as the use of a perthiolated βCD derivative as a capping ligand for the Au seeds. These gold nanojacks showed excellent electrocatalytic activity towards

H_2O_2, suggesting its potential use in analytical electrochemistry.

Acknowledgements

R. Villalonga acknowledges a Ramón & Cajal contract from the Spanish Ministry of Science and Innovation. Financial support from the Spanish Ministry of Science and Innovation (CTQ2011-24355 and CTQ2012-34238) and Comunidad de Madrid S2009/PPQ-1642, the programme AVANSENS, is gratefully acknowledged.

Notes and references

1 M. Grzelczak, J. Pérez-Juste, P. Mulvaney and L. M. Liz-Marzán, *Chem. Soc. Rev.*, 2008, **37**, 1783.
2 H. M. Chen, R. S. Liu and D. P. Tsai, *Cryst. Growth Des.*, 2009, **9**, 2079.
3 S. Barbosa, A. Agrawal, L. Rodríguez-Lorenzo, I. Pastoriza-Santos, R. A. Alvarez-Puebla, A. Kornowski, H. Weller and L. M. Liz-Marzán, *Langmuir*, 2010, **26**, 14943.
4 Z. Wang, L. Tang, L. H. Tan, J. Li and Y. Lu, *Angew. Chem., Int. Ed.*, 2012, **51**, 9078.
5 W. Wang and H. Cui, *J. Phys. Chem. C*, 2008, **112**, 10759.
6 L. Shao, A. S. Susha, L. S. Cheung, T. K. Sau, A. L. Rogach and J. Wang, *Langmuir*, 2012, **28**, 8979.
7 G. H. Jeong, Y. W. Lee, M. Kim and S. W. Han, *J. Colloid Interface Sci.*, 2009, **329**, 97.
8 C. L. Nehl, H. Liao and J. H. Hafner, *Nano Lett.*, 2006, **6**, 683.
9 T. K. Sau and C. J. Murphy, *J. Am. Chem. Soc.*, 2004, **126**, 8648.
10 E. Hao, R. C. Bailey, G. C. Schatz, J. T. Hupp and S. Li, *Nano Lett.*, 2004, **4**, 327.
11 P. Pallavicini, G. Chirico, M. Collini, G. Dacarro, A. Donà, L. D'Alfonso, A. Falqui, Y. Diaz-Fernandez, S. Freddi, B. Garofalo, A. Genovese, L. Sironi and A. Taglietti, *Chem. Commun.*, 2011, **47**, 1315.
12 X. Zou, E. Ying and S. Dong, *Nanotechnology*, 2006, **17**, 4758.
13 L. Vigderman and E. R. Zubarev, *Langmuir*, 2012, **28**, 9034.
14 S. Bernhardt, P. Glöckner, A. Theis and H. Ritter, *Macromolecules*, 2001, **34**, 1647.
15 Y. Liu, K. B. Male, P. Bouvrette and J. H. T. Luong, *Chem. Mater.*, 2003, **15**, 4172.
16 F. S. Damos, R. C. S. Luz, A. A. Tanaka and L. T. Kubota, *Anal. Chim. Acta*, 2010, **664**, 144.
17 J. Liu, W. Ong, E. Román, M. J. Lynn and A. E. Kaifer, *Langmuir*, 2000, **16**, 3000.
18 R. Villalonga, A. Fragoso, R. Cao, P. D. Ortiz, M. L. Villalonga and A. E. Damiao, *Supramol. Chem.*, 2005, **17**, 387.
19 I. Baussanne, H. Law, J. Defaye, J. M. Benito, C. Ortiz Mellet and J. M. García Fernández, *Chem. Commun.*, 2000, 1489.
20 M. T. Rojas, R. Koeniger, J. F. Stoddart and A. E. Kaifer, *J. Am. Chem. Soc.*, 1995, **117**, 336.
21 B. Nikoobakht and M. A. El-Sayed, *Chem. Mater.*, 2003, **15**, 1957.
22 F. Hao, C. L. Nehl, J. H. Hafner and P. Nordlander, *Nano Lett.*, 2007, **7**, 729.
23 Q. Su, X. Ma, J. Dong, C. Jiang and W. Qian, *ACS Appl. Mater. Interfaces*, 2011, **3**, 1873.
24 M. R. Langille, M. L. Personick, J. Zhang and C. A. Mirkin, *J. Am. Chem. Soc.*, 2012, **134**, 14542.
25 M. Liu and P. Guyot-Sionnest, *J. Phys. Chem. B*, 2005, **109**, 22192.
26 N. Garg, C. Scholl, A. Mohanty and R. Jin, *Langmuir*, 2010, **26**, 10271.
27 J. S. DuChene, W. Niu, J. M. Abendroth, Q. Sun, W. Zhao, F. Huo and W. D. Wei, *Chem. Mater.*, 2013, **25**, 1392.
28 W. Chen, S. Cai, Q. Q. Ren, W. Wena and Y. D. Zhao, *Analyst*, 2012, **137**, 49.
29 T. Masadome, A. Ueda and M. Kawakami, *Anal. Lett.*, 2004, **37**, 225.
30 R. Hosseinzadeh, R. E. Sabzi and K. Ghasemlu, *Colloids Surf., B*, 2009, **68**, 213.

